

# Thermally Stable Nanocrystalline Aluminum Alloys Processed by Mechanical Alloying and High Frequency Induction Heat Sintering

Hany R. Ammar, Khalil A. Khalil, El-Sayed M. Sherif

**Abstract**—The current study investigated the influence of milling time and ball-to-powder (BPR) weight ratio on the microstructural constituents and mechanical properties of bulk nanocrystalline Al; Al-10%Cu; and Al-10%Cu-5%Ti alloys. Powder consolidation was carried out using a high frequency induction heat sintering where the processed metal powders were sintered into a dense and strong bulk material. The powders and the bulk samples were characterized using XRD and FEGSEM techniques. The mechanical properties were evaluated at various temperatures of 25°C, 100°C, 200°C, 300°C and 400°C to study the thermal stability of the processed alloys. The processed bulk nanocrystalline alloys displayed extremely high hardness values even at elevated temperatures. The Al-10%Cu-5%Ti alloy displayed the highest hardness values at room and elevated temperatures which are related to the presence of Ti-containing phases such as Al<sub>3</sub>Ti and AlCu<sub>2</sub>Ti. These phases are thermally stable and retain the high hardness values at elevated temperatures up to 400°C.

**Keywords**—Nanocrystalline Aluminum Alloys, Mechanical Alloying, Sintering, Hardness, Thermal Stability.

## I. INTRODUCTION

**M**echanical Alloying (MA) is a solid-state powder processing technique which involves repeated welding, fracturing, and re-welding of powder particles in a high-energy ball mill. A variety of equilibrium and non-equilibrium alloy phases could be synthesized using mechanical alloying starting from elemental powders. Several advantages could be attained when using MA in materials production. These benefits include: production of fine dispersoid of second phase particles; extending the equilibrium solid solubility limit; refining the grain sizes to the nanoscale; producing new phases; and alloying of immiscible alloying elements [1]-[5].

The processing parameters involved in mechanical alloying technique require a suitable control to attain the desired properties of the mechanically alloyed products. These are some significant variables which influence the properties of the processed products: speed of milling, time of milling,

grinding medium, ball-to-powder weight ratio, extent of filling the container, atmosphere of milling, process control agent, and milling temperature. Optimizing the previously-mentioned variables is a critical process for achieving the desired properties/microstructure of the produced alloys [6].

Several aluminum alloys have been already developed using mechanical alloying such as Al-Mg, Al-Ti and Al-Zr alloys. High strength Al-Ti alloys have been recently developed for elevated temperatures applications using mechanical alloying by dispersing nano/submicron scale Al<sub>3</sub>Ti particles in an Al matrix [7], [8]. Al-Fe alloys are another series of thermally stable aluminum alloys with superior mechanical and physical properties even at elevated temperatures. This particular alloy system is successfully developed and produced using mechanical alloying technique [9]-[12].

The current research project aims at developing thermally stable aluminum alloys by designing new compositions of Al alloys. The design of the new alloys will be achieved by adding low diffusivity alloying elements such as Ti. This particular alloying element displays low solubility in aluminum even at elevated temperatures. Mechanical alloying technique will be used for producing these alloys to make use of the advantages of this technique, specifically, extension of solid solubility; refining grain sizes to nanoscale and formation of thermally stable second phase particles. The extension of solid solubility of the low diffusivity elements, such as Ti, in aluminum will give the chance for forming a thermally stable nanosized precipitates such as Al<sub>3</sub>Ti [13], [14].

## II. EXPERIMENTAL PROCEDURES

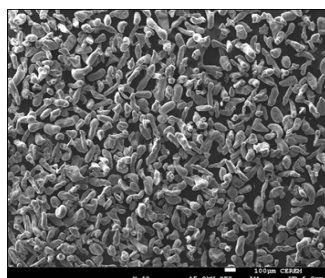
The as-received metal powders were used to synthesis nanocrystalline Al, Al-10%Cu, and Al-10%Cu-5%Ti alloys using mechanical alloying technique. High purity Al, Cu and Ti metal powders (purity > 99.9%) with an average particles size of 100 microns were used. Stearic acid was used as a process control agent to maintain the balance between cold welding and fracturing of powder particles and to prevent powders agglomeration, an amount of 5 wt% of stearic acid was added to the powders mixtures. Fig. 1 shows the morphology of the processed powders where Fig. 1 (a) illustrates the morphology of the as-received aluminum powders while Figs. 1 (b) and (c) show the morphology of mechanically alloyed Al-10%Cu powders for 6 h at low and high magnification, respectively.

Hany R. Ammar is with Metallurgical and Materials Engineering Department, Faculty of Petroleum and Mining Engineering, Suez University, Suez, 43721, Egypt, (Corresponding Author, Tel: +201204615626, e-mail: Hany\_Ammar@uqac.ca)

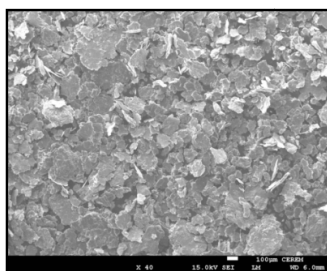
Khalil A. Khalil is with Mechanical Engineering Department, College of Engineering, King Saud University, P.O. Box 800, Riyadh, 11421 (e-mail: kabdelmawgoud@ksu.edu.sa).

El-Sayed M. Sherif is with Center of Excellence for Research in Engineering Materials (CEREM), Advanced Manufacturing Institute, King Saud University, P. O. Box 800, Al-Riyadh 11421, Saudi Arabia, (e-mail: esherif@ksu.edu.sa).

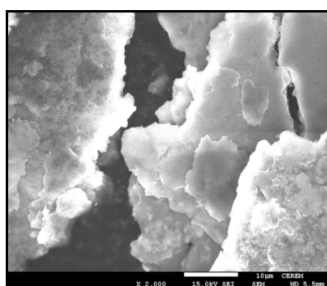
The current study investigated the influence of processing parameters on the microstructure and hardness values of the produced materials at room and elevated temperatures. Two milling times of 3 and 6 hours were applied and ball-to-powders weight ratio (BPR) of 30:1 and 90:1 were also applied to investigate their effects on the microstructure and hardness values of the processed alloys. The mechanical alloying process was carried out using 1S-attritor. The milling process was undertaken under argon atmosphere to avoid any contamination of the processed powders from the atmosphere.



(a)



(b)

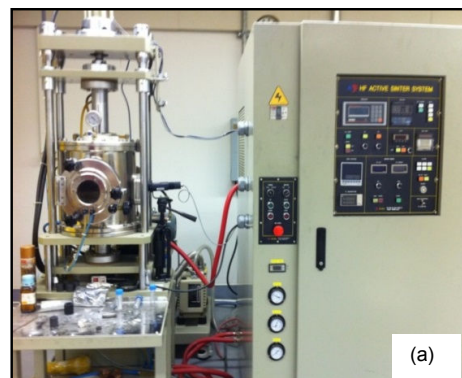


(c)

Fig. 1 Morphology of the processed powders: (a) as-received aluminum powders; (b) mechanically alloyed Al-10%Cu powders for 6 h; and (c) mechanically alloyed Al-10%Cu powders for 6 h at higher magnification

Powder consolidation was carried out using a high frequency induction heat sintering machine, as shown in Fig. 2 (a), where the processed alloys powders were sintered into a dense and strong bulk material. The sintering conditions applied in this process were heating rate of 350°C/min; sintering time of 4 minutes; sintering temperature of 400°C; applied pressure of 750 Kg/cm<sup>2</sup> (74 MPa); cooling rate of

400°C/min and the process was carried under vacuum of 10<sup>-3</sup> Torr. The processed powders were placed in a graphite die and then introduced into the high-frequency induction heat sintering (HFIHS). The basic configuration of a HFIHS unit is shown in Fig. 2.



(a)

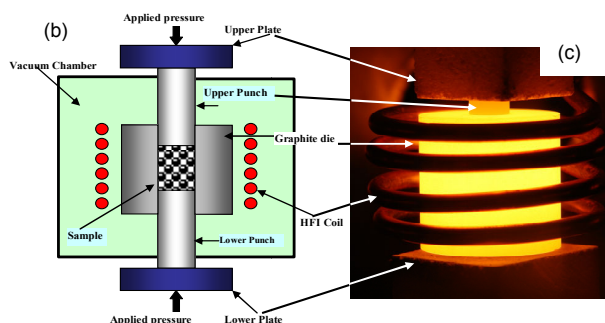


Fig. 2 (a) High frequency induction heat sintering machine used for powder compaction in the present study, (b) Schematic diagram of high-frequency induction heated sintering apparatus, and (c) an image of the heated die

HFIHS consists of a uniaxial pressure device and a graphite die (outside diameter, 45 mm; inside diameter, 10 mm; and height, 40 mm). The unit also features a water-cooled reaction chamber that can be evacuated, an induced current (frequency of approximately 50 kHz) and pressure-, position- and temperature-regulating systems. HFIHS resembles the hot pressing process in several respects, i.e., the precursor powder is loaded in a die and a uniaxial pressure is applied during the sintering process. However, instead of using an external heating source, an intensive magnetic field is applied through the electrically conducting pressure die and, in some cases, also through the sample. This implies that the die also acts as a heating source and that the sample is heated from both the outside and inside. Temperatures can be measured whether by a pyrometer focused on the surface of the graphite die or by thermocouple inserted in a hole in the surface of the die. The system is first evacuated to a vacuum level of 1 × 10<sup>-3</sup> Torr, and a uniaxial pressure is applied. An induced current (frequency of approximately 50 kHz) is then activated and maintained until densification is observed, indicating the occurrence of sintering and the concomitant shrinkage of the

sample. Sample shrinkage is measured by a linear gauge that measures the vertical displacement.

X-Ray Diffraction (XRD) technique was used for the purpose of evaluating the mechanically alloyed powders and the sintered bulk samples. Crystallite size, lattice strain, and phases formed before and after sintering were characterized using XRD technique. It should be noted that the crystallite size was determined by XRD data and Scherrer equation.

Field emission gun scanning electron microscope (FEGSEM) was used for characterizing the microstructural constituents of the sintered samples. The sintered bulk samples were solution heat treated at 450°C for 3 hours before performing the hardness testing. Mechanical properties evaluation was undertaken using Vickers hardness test with a force of 10 Kgf and dwell time of 15 sec. The hardness test was carried out at various temperatures of 25°C, 100°C, 200°C, 300°C and 400°C to characterize the high temperature mechanical properties of the produced alloys.

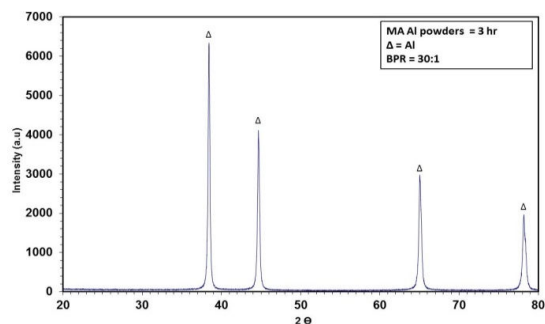
### III. RESULTS & DISCUSSION

The main objective of the current study is to synthesize thermally stable aluminum alloys using mechanical alloying technique. Three alloys compositions were investigated in the present study: pure aluminum; Al-10%Cu; and Al-10%Cu-5%Ti. Two parameters of the mechanical alloying technique were studied: the influence of milling time of 3 and 6 hours and the effect of ball-to-powder weight ratio (BPR) of 30:1 and 90:1. Figs. 3-5 illustrate the XRD patterns of mechanically alloyed Al-powders under various milling time and BPR. From an analysis of these XRD patterns, it may be observed that increasing the milling time results in refining the crystallite size, as may be observed from the broadening of the XRD patterns. Also, increasing the milling time results in dissolving the alloying elements of Cu and Ti in the Al-matrix.

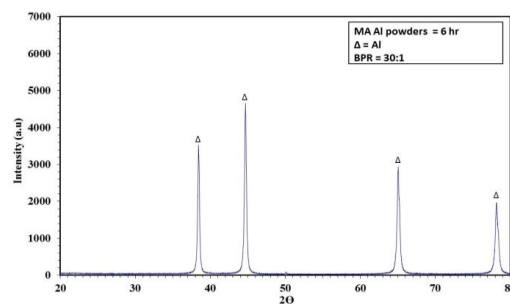
Fig. 3 (a) shows the XRD pattern of pure aluminum powders mechanically alloyed for 3 h using BPR of 30:1. Fig. 3 (b) shows the pattern of the aluminum powders milled for 6 h and BPR was 30:1, increasing the milling time results in reducing the crystallite size from 62 nm to 57 nm. Figs. 3 (c) and (d) illustrate the XRD patterns of pure aluminum milled for 3 and 6 h, respectively, under the effect of larger BPR of 90:1. This large BPR results in a further reduction in the crystallite size of aluminum down to 18 nm due to the strong collision force between the balls and the powders and the high energy input when increasing the BPR to 90:1.

Figs. 4 (a) and (b) show the XRD patterns of mechanically alloyed Al-10%Cu powders mechanically milled for 3 h and 6 h, respectively, using BPR of 30:1. Increasing the milling time results in reducing the crystallite size from 68 nm to 50 nm. Figs. 4 (c) and (d) show the XRD patterns of mechanically alloyed Al-10%Cu powders for 3 h and 6 h, respectively, milling was carried out using BPR of 90:1. Increasing both the BPR to 90:1 and the time to 6 h results in a complete dissolution of Cu in aluminum matrix, as it may be observed in Fig. 4 (d), all Cu-peaks disappeared due to complete dissolution of Cu in Al. In addition, these conditions result in a

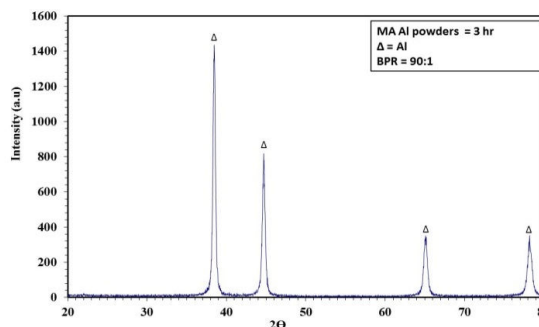
further reduction in the crystallite size of Al-10%Cu alloy down to 14 nm.



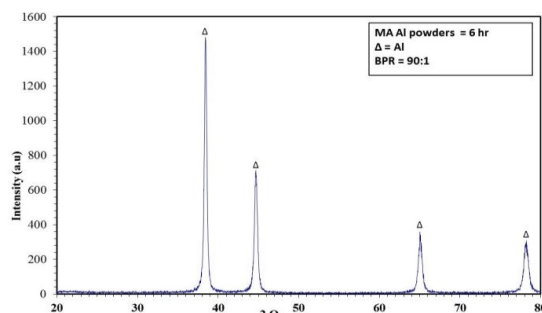
(a)



(b)



(c)



(d)

Fig. 3 XRD patterns of mechanically alloyed Al-powders: (a) BPR of 30:1 and milling time of 3 h; (b) BPR of 30:1 and milling time of 6 h; (c) BPR of 90:1 and milling time of 3 h; and (d) BPR of 90:1 and milling time of 6 h

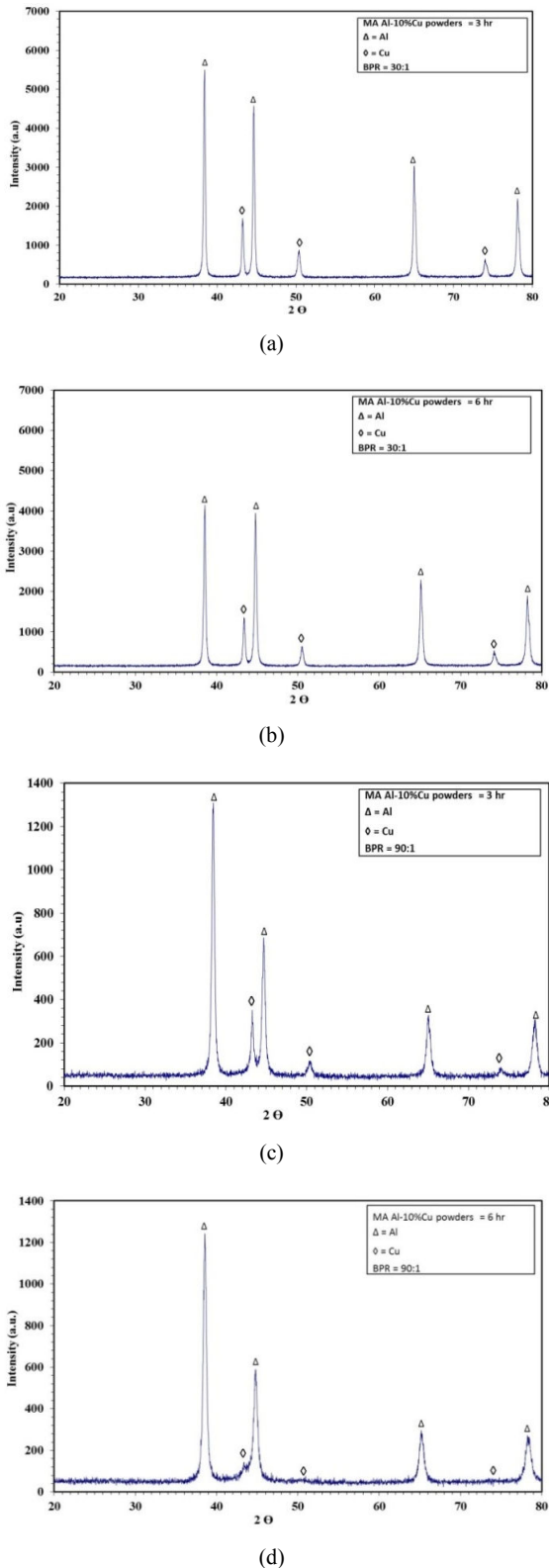


Fig. 4 XRD patterns of mechanically alloyed Al-10%Cu powders: (a) BPR of 30:1 and milling time of 3 h; (b) BPR of 30:1 and milling time of 6 h; (c) BPR of 90:1 and milling time of 3 h; and (d) BPR of 90:1 and milling time of 6 h

Figs. 5 (a) and (b) show the XRD patterns of mechanically alloyed Al-10%Cu-5%Ti powders for 3 h and 6 h, respectively, milling was carried out using BPR of 90:1. Similar observations were noted from these patterns where the large balls to powders weight ratio and the longer milling time result in a complete solubility of the alloying elements, namely, Cu and Ti in the Al matrix and also reducing the crystallite size down to 12 nm.

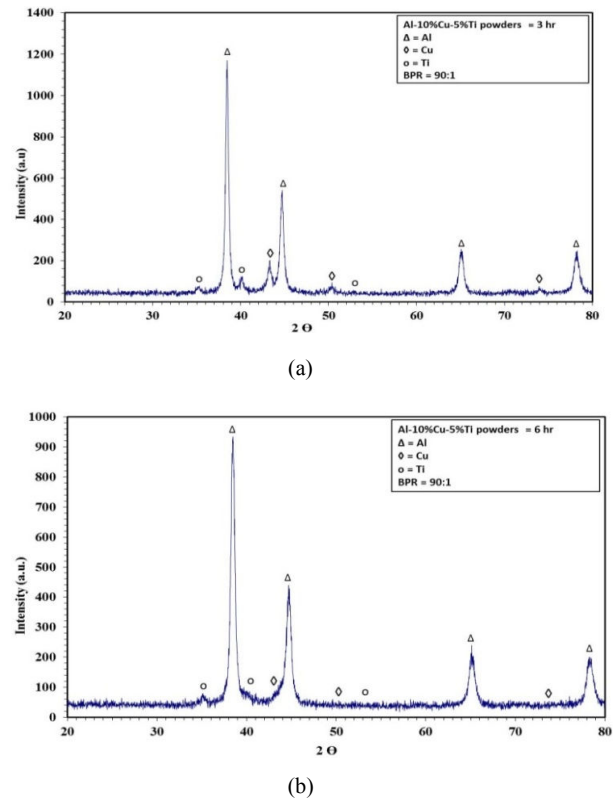


Fig. 5 XRD patterns of mechanically alloyed Al-10%Cu-5%Ti powders, BPR = 90:1; milling time (a) 3 h and (b) 6 h

Figs. 6 and 7 summarize the influence of milling parameters on the crystallite size and lattice strain of the mechanically alloyed Al-alloys. Increasing milling time reduces the grain size and increases the lattice strain. Increasing the ball-to-powder weight ratio results in a further decrease in the grain size and an additional increase in the lattice strain.

Powders consolidation was carried out using a high frequency sintering machine where the processed alloys powders were sintered into a dense and strong bulk samples. The parameters applied to the sintering process were as follow: heating rate of  $350^\circ\text{C}/\text{min}$ ; sintering time of 4 minutes; sintering temperature of  $400^\circ\text{C}$ ; applied pressure of  $750 \text{ Kg}/\text{cm}^2$  (74 MPa); and the compaction process was carried out under vacuum of  $10^{-3}$  Torr. The selected powders for sintering process were those powders subjected to milling time for 6 hours and BPR of 90:1. This selection was made based on the idea that these conditions produced the finest crystallite size of the three alloys.

Figs. 6 and 7 illustrate that the powders consolidation process results in an increase in the grain size and a decrease in lattice strain which are related to the effect of applying high temperature of 400°C for sintering process. This high

temperature leads to a grain growth which produces relatively coarser grain size and also leads to a release of the internal stress which produces low level of lattice strain.

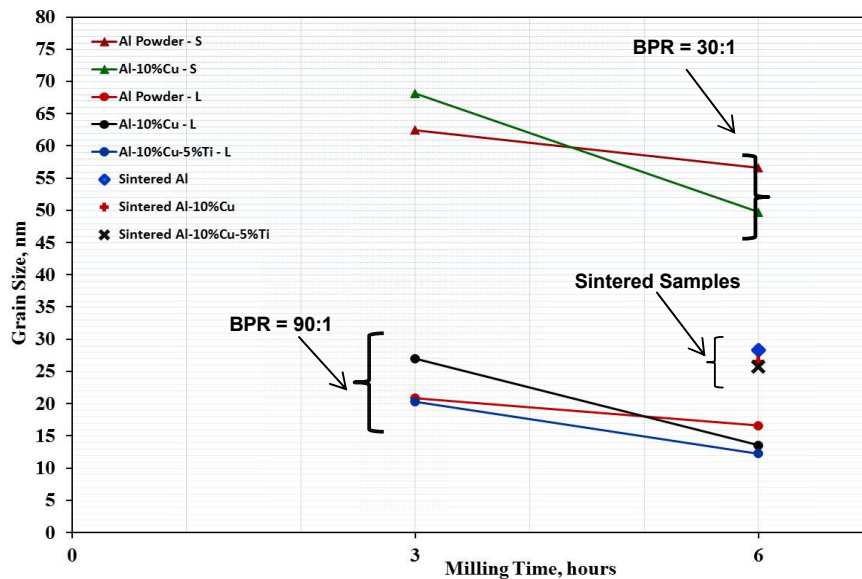


Fig. 6 Crystallite size obtained for the mechanically alloyed Al-alloys under various milling time and BPR

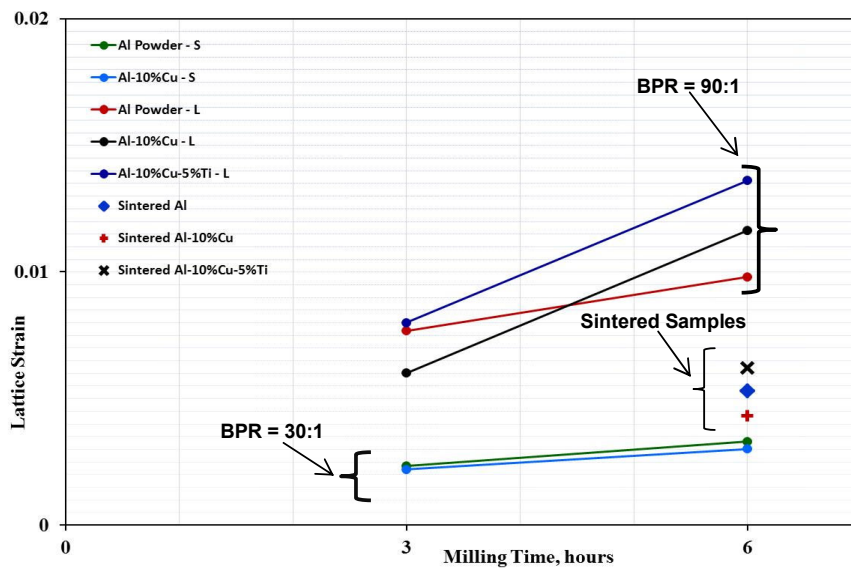


Fig. 7 Lattice strain obtained for the mechanically alloyed Al-alloys under various milling time and BPR

Fig. 8 shows the XRD patterns obtained for the solid bulk samples. Fig. 8 (a) shows the XRD pattern for pure aluminum bulk sample, the crystallite size was observed to increase from 18 nm to 28 nm after sintering process, in addition, the XRD pattern shows that there is a peak for  $\text{Al}_2\text{O}_3$  which formed during sintering process. Fig. 8 (b) illustrates the XRD pattern for Al-10%Cu bulk sample, the grain size was observed to increase from 14 nm to 27 nm after sintering process. The XRD pattern shows the main second phases formed after sintering.  $\text{Al}_2\text{Cu}$  phase was observed to form in the aluminum

matrix after sintering process. The microstructure of Al-10%Cu alloy is shown in Fig. 9 where Fig. 9 (a) shows the SEM image at 1200x showing the uniform distribution of the hardening phases of  $\text{Al}_2\text{Cu}$  formed in the matrix after sintering. Fig. 9 (b) shows SEM image at 10000x showing ultrafine precipitates of  $\text{Al}_2\text{Cu}$  phases. The EDX analysis shown in Fig. 9 (c) conform the main elements of the phases observed in Fig. 9 (b).

Fig. 8 (c) shows the XRD pattern for Al-10%Cu-5%Ti, as observed before, the grain size was observed to increase from



12 nm to 28 nm after sintering process. The XRD pattern illustrates the main second phases formed in this alloy after sintering. The second phases formed in this alloy, as shown in the XRD pattern, are  $\text{Al}_2\text{Cu}$ ,  $\text{Al}_3\text{Ti}$ , and  $\text{AlCu}_2\text{Ti}$ . These phases are also observed in the SEM images shown in Fig. 10 where Fig. 10 (a) shows the microstructure at low magnification illustrating a variety of phases formed in the matrix after

sintering. Fig. 10 (b) illustrates the main phases at higher magnification where three main phases were observed in the matrix as confirmed by the EDX analysis shown in Figs. 10 (c)-(e). The EDX analysis confirmed the formation of the phases observed in the XRD pattern shown in Fig. 10 (c). The three phases observed in the Al-10%Cu-5%Ti alloy are  $\text{Al}_2\text{Cu}$ ,  $\text{Al}_3\text{Ti}$ , and  $\text{AlCu}_2\text{Ti}$ .

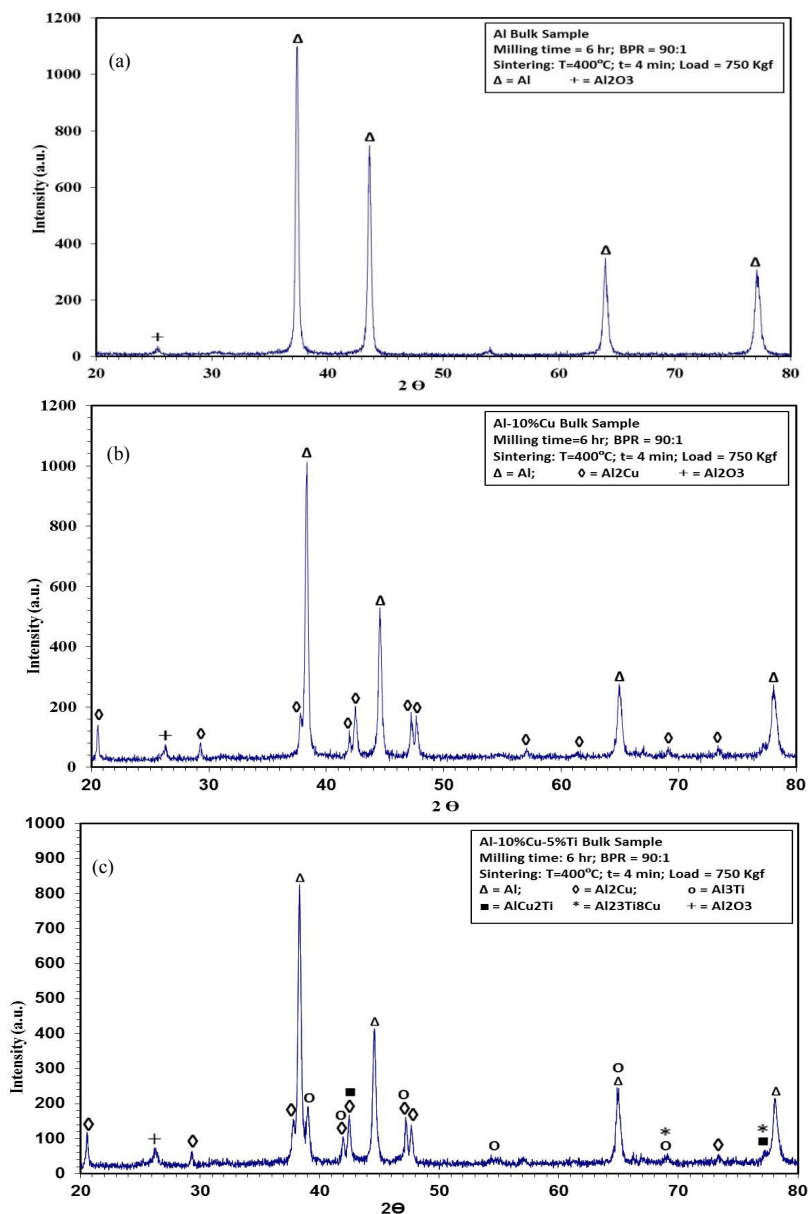
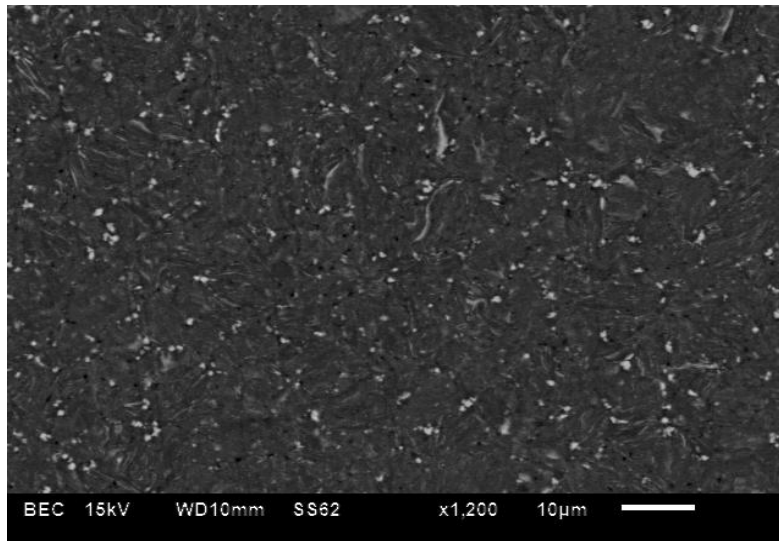
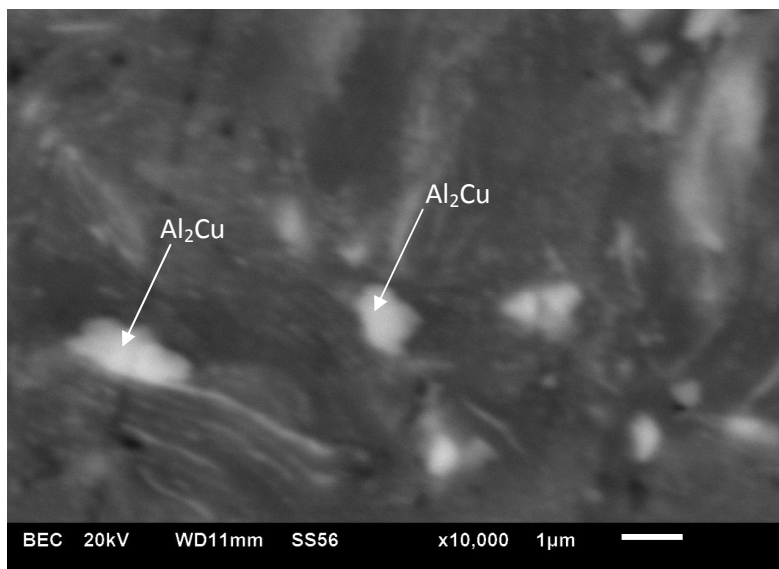


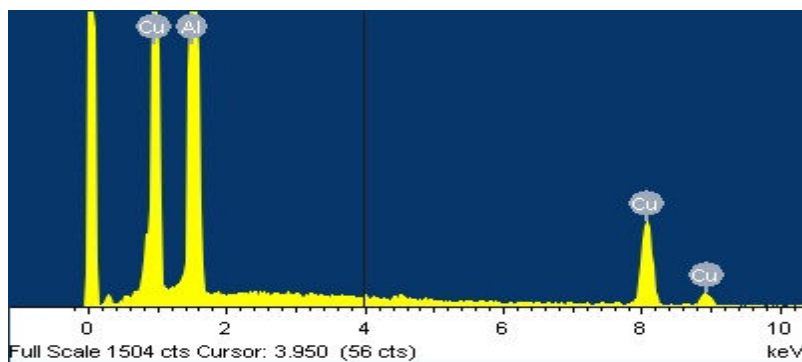
Fig. 8 XRD patterns of sintered bulk samples mechanically alloyed for 6 h and BPR = 90:1 (a) pure Al; (b) Al-10%Cu alloy; and (c) Al-10%Cu-5%Ti alloy



(a)

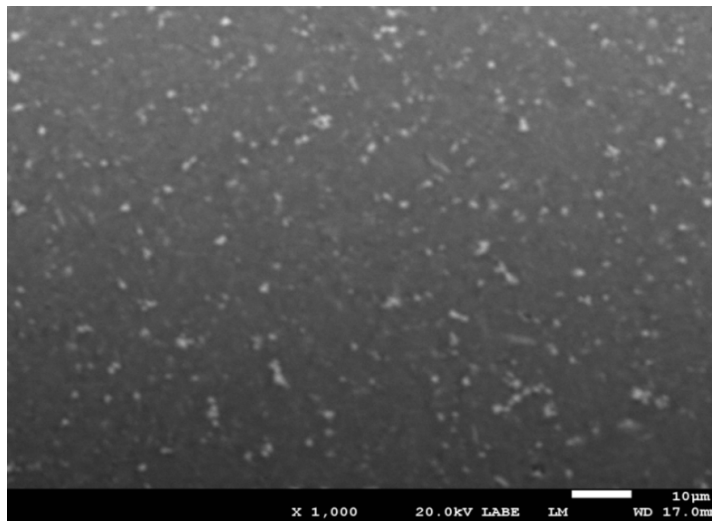


(b)

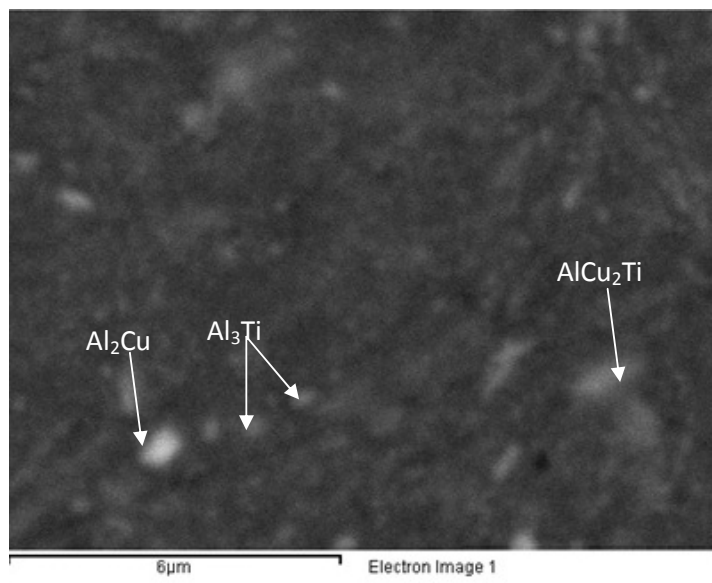


(c)

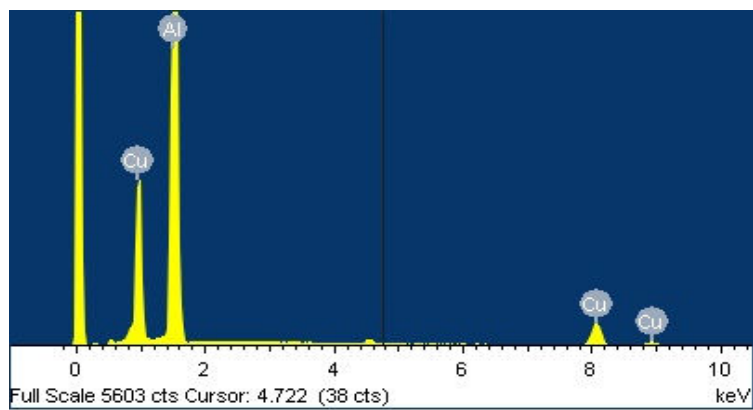
Fig. 9 (a) SEM image at 1200x showing the microstructure of Al-10%Cu; (b) SEM image at 10000x showing  $Al_2Cu$  phases; and (c) an EDX spectrum illustrating the main elements of phases observed in (b)



(a)

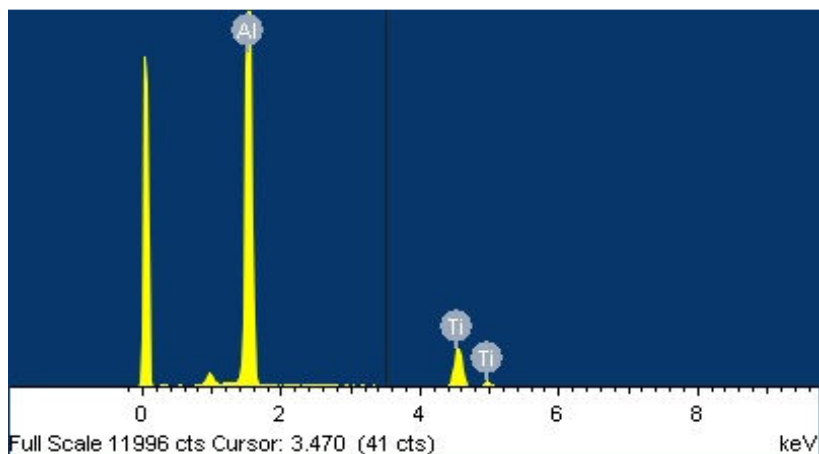


(b)

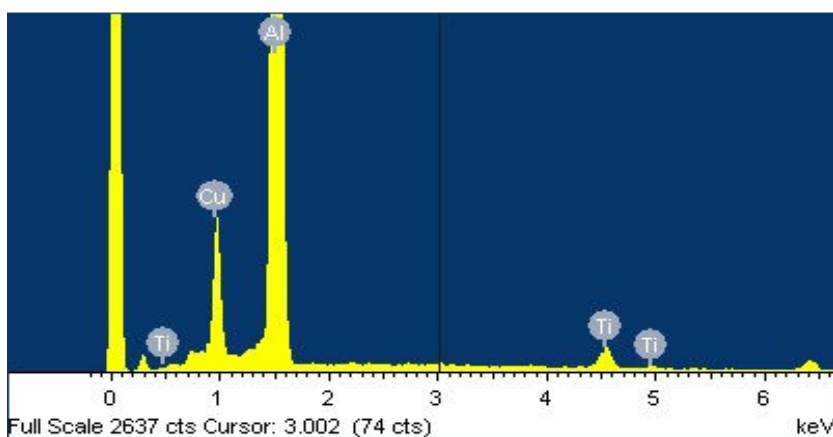


(c)





(d)



(e)

Fig. 10 (a) SEM image at low magnification showing the microstructure of Al-10%Cu-5%Ti; (b) SEM image at higher magnification showing  $\text{Al}_2\text{Cu}$ ,  $\text{Al}_3\text{Ti}$  and  $\text{AlCu}_2\text{Ti}$  phases. (c), (d) and (e) EDX spectrums illustrating the main elements of phases observed in (b)

The hardness test was carried out at different test temperatures for the purpose of evaluating the mechanical properties of the produced alloys at elevated temperatures. Vickers hardness test was performed with an applied force of 10 Kgf and dwell time of 15 second. An average of five hardness values were measured for each sample at random five points. The hardness test results of the alloys under study are presented in Table I and Fig. 11. The bulk samples of the alloys under study were first tested at room temperature (25°C) in the as-sintered (A.S.) condition and after applying solution heat treatment (S.H.T.) at 450°C for 3 hours followed by water quenching. According to the results shown in Table I and Fig. 11, the solution heat treated samples displayed higher hardness values as compared to the as-sintered samples. Accordingly, the hardness test was performed on the solution heat treated samples at four different temperatures of 100°C; 200°C; 300°C; and 400°C.

From the results shown in Table I and Fig. 11, it may be observed that the three alloys displayed extremely high hardness values after solutionizing. The hardness value at

room temperature of heat treated bulk samples processed by mechanical alloying of pure Al, Al-10%Cu, and Al-10%Cu-5%Ti are 124, 259, and 331, respectively. These hardness values are extremely high due to the nanocrystalline structure of these alloys and also the formation of the ultra-fine hardening phases. The hardness in case of pure aluminum is related mainly to the nanocrystalline structure which significantly improves the strength of pure aluminum. In case of Al-10%Cu, the hardness is higher than that of pure aluminum due to the formation of the hardening phases of  $\text{Al}_2\text{Cu}$  on the ultra-fine scale, as shown in Fig. 9.

Regarding Al-10%Cu-5%Ti alloy, it displayed the highest hardness values as may be observed in Table I and Fig. 11, which is related to the nanocrystalline structure and the formation of several hardening phases on the ultra-fine scale such as  $\text{Al}_2\text{Cu}$ ,  $\text{Al}_3\text{Ti}$  and  $\text{AlCu}_2\text{Ti}$ , as illustrated in Fig. 10. The mechanically alloyed samples displayed extremely high hardness values even at high temperatures. The hardness values at 400°C of pure Al, Al-10%Cu, and Al-10%Cu-5%Ti alloys were observed as 68, 86, and 122 respectively. These

hardness values at 400°C are considered as large values when compared to the hardness of conventional aluminum alloys [15]. It may be observed that the Al-10%Cu-5%Ti alloy displayed the best thermal stability of the mechanical properties at elevated temperatures which is related to the formation of fine dispersoid of second phase particles such as  $Al_3Ti$  and  $AlCu_2Ti$ . These Ti-containing phases are thermally stable at elevated temperatures due to the limited solubility of Ti in the aluminum matrix which prevents these phases from

dissolution or coarsening. In addition, mechanical alloying technique results in extending the equilibrium solubility limit of Ti in Al which forms super-saturated solid solution of Ti in Al matrix and this provides further increase in the strength even at elevated temperatures. Furthermore, the mechanical alloying process results in refining the grain sizes to the nanoscale which results in a further enhancement in the hardness of these alloys.

TABLE I  
VICKERS HARDNESS VALUES OBTAINED IN THE CURRENT STUDY FOR PURE AL, AL-10%CU AND AL-10%CU-5%TI PROCESSED BY MECHANICAL ALLOYING (BPR = 90:1 AND MILLING TIME OF 6 HRS).

| Condition    | Vickers Hardness |      |          |     |               |     |
|--------------|------------------|------|----------|-----|---------------|-----|
|              | Pure Al          |      | Al-10%Cu |     | Al-10%Cu-5%Ti |     |
|              | Average          | ±SD* | Average  | ±SD | Average       | ±SD |
| A.S.*(25°C)  | 97               | 2    | 239      | 4   | 303           | 3   |
| S.H.T*(25°C) | 124              | 9    | 259      | 3   | 331           | 9   |
| 100°C        | 117              | 5    | 231      | 2   | 289           | 4   |
| 200°C        | 98               | 2    | 165      | 6   | 194           | 9   |
| 300°C        | 85               | 3    | 125      | 9   | 164           | 4   |
| 400°C        | 68               | 2    | 86       | 5   | 122           | 9   |

SD refers to standard deviation; A.S. indicates as-sintered; and S.H.T. refers to annealed.

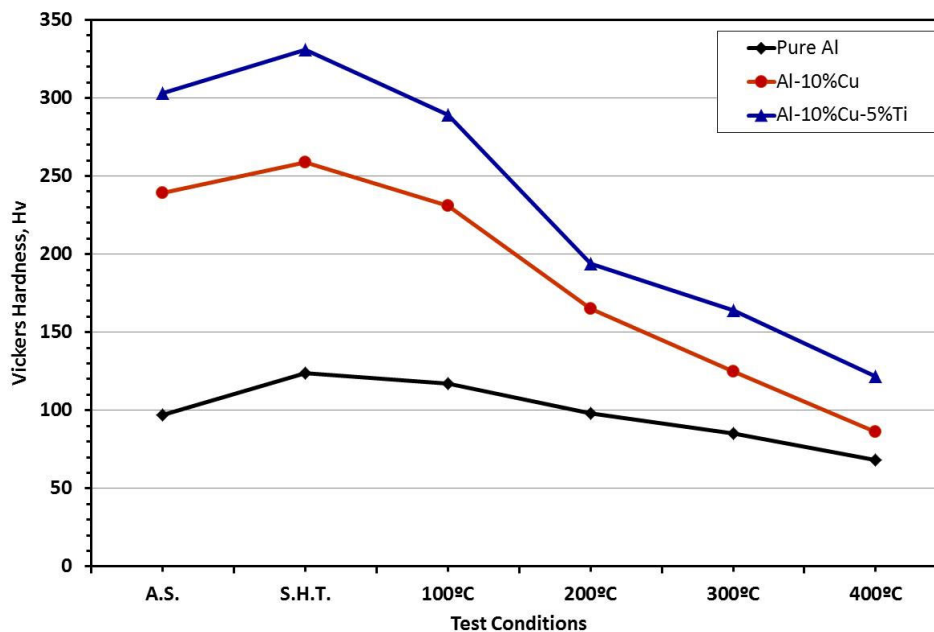


Fig. 11 Vickers hardness values for pure Al, Al-10%Cu and Al-10%Cu-5%Ti processed by mechanical alloying (BPR of 90:1 and milling time of 6 hrs). The hardness test of the solution heat treated samples was carried out at 25°C, 100°C, 200°C, 300°C, and 400°C

#### IV. CONCLUSIONS

1. The production of Al alloys using mechanical alloying technique resulted in several advantages such as extension of solid solubility limit of Ti in Al; forming a super saturated solid solution of Cu and Ti in Al matrix for Al-10%Cu and Al-10%Cu-5%Ti alloys, respectively; refinement of crystallite size down to nanometer scale (the minimum size obtained was 12 nm); and formation of thermally stable phases such as  $Al_3Ti$  and  $AlCu_2Ti$  which provide high strength even at elevated temperatures.
2. Increasing the milling time from 3 hours to 6 hours resulted in more refining in the crystallite size; increasing lattice strains; and extending the solubility limit of Ti and Cu in Al matrix.
3. Increasing the ball-to-powder weight ratio from 30:1 to 90:1 resulted in more refining in the crystallite size; further increase in the lattice strains; and more extension in the solubility limit of Ti and Cu in Al matrix.
4. The sintering process is a critical step in forming the bulk solid samples. High frequency induction heat sintering

technique was successfully applied in producing bulk solid dense samples.

5. The matrix of the bulk solid samples contains several hardening phases such as Al<sub>2</sub>Cu in Al-10%Cu alloy and Al<sub>2</sub>Cu, Al<sub>3</sub>Ti, AlCu<sub>2</sub>Ti in case of Al-10%Cu-5%Ti alloy. These phases are considered as one of the basic source of strengthening the alloys under study.
6. The sintered samples displayed extremely high Vickers hardness values at room and elevated temperatures. The Al-10%Cu-5%Ti alloy displayed the highest hardness values at room and elevated temperatures which are related to the presence of Ti-containing phases such as Al<sub>3</sub>Ti and AlCu<sub>2</sub>Ti, these phases are thermally stable and retain the high hardness values at elevated temperatures up to 400°C.

[15] *ASM Handbook Vol. 2, "Properties and selection: nonferrous alloys and special-purpose materials,"* ASM International, Materials Information Society, U.S.A., 1990.

#### ACKNOWLEDGMENT

This project was supported by NSTIP strategic technologies program number (11-ADV1853-02) in the Kingdom of Saudi Arabia.

#### REFERENCES

- [1] C.C. Koch, "Intermetallic matrix composites prepared by mechanical alloying - a review," *Materials Science and Engineering*, Vol. A244, 1998, pp. 39-48.
- [2] H.D.K.H, "Mechanically alloyed metals," *Materials Science and Technology*, Vol. 1, 2000, pp. 1404-1411.
- [3] M.A. Shaikh, M. Iqbal, J.I. Akhter, M. Ahmad, Q. Zaman, M. Akhtar, M.J. Moughal, Z. Ahmed, and M. Farooque, "Alloying of immiscible Ge with Al by ball milling," *Materials Letters*, Vol. 57, 2003, pp. 3681-3685.
- [4] E. Ma and M. Atzmon, "Phase transformations induced by mechanical alloying in a binary system," *Materials Chemistry and Physics*, Vol. 39, 1995, pp. 249-267.
- [5] C.C. Koch and J.D. Whittenberger, "Review: mechanical milling/alloying of Intermetallic," *Intermetallics*, Vol. 4, 1996, pp. 339-355.
- [6] C. Suryanarayana, "Mechanical alloying and milling," *Progress in Materials Science*, Vol. 46, 2001, pp. 1-184.
- [7] Kwang-Min Lee and In-Hyung Moon, "High temperature performance of dispersion-strengthened Al-Ti alloys prepared by mechanical alloying," *Materials Science and Engineering*, Vol. A 185, 1994, pp. 165-170.
- [8] R. Lurf and D. G. Morris, "Mechanical alloying of Al-Ti alloys," *Materials Science and Engineering*, Vol. A 128, 1990, pp. 119-127.
- [9] L. Shaw, H. Luo, J. Villegas and D. Miracle, "Thermal stability of nanostructured Al<sub>93</sub>Fe<sub>3</sub>Cr<sub>2</sub>Ti<sub>2</sub> alloys prepared via mechanical alloying," *Acta Materialia*, Vol. 51, 2003, pp. 2647-2663.
- [10] T.T. Sasaki, T. Ohkubo and K. Hono, "Microstructure and mechanical properties of bulk nanocrystalline Al-Fe alloy processed by mechanical alloying and spark plasma sintering," *Acta Materialia*, Vol. 57, 2009, pp. 3529-3538.
- [11] T.T. Sasaki, T. Mukai and K. Hono, "A high-strength bulk nanocrystalline Al-Fe alloy processed by mechanical alloying and spark plasma sintering," *Scripta Materialia*, Vol. 57, 2007, pp. 189-192.
- [12] M. Krasnowski and T. Kulik, "Nanocrystalline and amorphous Al-Fe alloys containing 60-85% of Al synthesized by mechanical alloying and phase transformations induced by heating of milling products," *Materials Chemistry and Physics*, Vol. 116, 2009, pp. 631-637.
- [13] K.I. Moon and K.S. Lee, "Compressive deformation behavior of nanocrystalline Al-5at.% Ti alloys prepared by reactive ball milling in H and ultra-high-pressure hot pressing," *Journal of Alloys and Compounds*, Vol. 333, 2002, pp. 249-259.
- [14] K.I. Moon and K.S. Lee, "Development of nanocrystalline Al-Ti alloy powders by reactive ball milling," *Journal of Alloys and Compounds*, Vol. 264, 1998, pp. 258-266.